Multi-dimensional visualization for the morphology of lubricant stearic acid particles and their distribution in tablets

Liu Zhang , Shailendra Shakya , Li Wu , Jiangtao Wang , Guanghui Jin , Huimin Sun , Xianzhen Yin , Lixin Sun , Jiwen Zhang

PII: S1818-0876(18)30779-7
DOI: https://doi.org/10.1016/j.ajps.2019.01.001
Reference: AJPS 586

To appear in: *Asian Journal of Pharmaceutical Sciences*

Received date: 29 July 2018
Revised date: 18 November 2018
Accepted date: 10 January 2019

Please cite this article as: Liu Zhang , Shailendra Shakya , Li Wu , Jiangtao Wang , Guanghui Jin , Huimin Sun , Xianzhen Yin , Lixin Sun , Jiwen Zhang , Multi-dimensional visualization for the morphology of lubricant stearic acid particles and their distribution in tablets, *Asian Journal of Pharmaceutical Sciences* (2019), doi: https://doi.org/10.1016/j.ajps.2019.01.001

Original Reseach Paper

Multi-dimensional visualization for the morphology of lubricant stearic acid particles and their distribution in tablets

Liu Zhang[a,b], Shailendra Shakya[b] , Li Wu[b], Jiangtao Wang[c], Guanghui Jin[c], Huimin Sun[d], Xianzhen Yin[b,*], Lixin Sun[a,**], Jiwen Zhang[a,b,*]

[a] School of Pharmacy, Shenyang Pharmaceutical University, Shenyang 110016, China;

[b] Center for Drug Delivery Systems, Shanghai Institute of Materia Medica, Chinese Academy of Sciences, Shanghai 201203, China;

[c] Weihai Disu Pharmaceutical Manufacturer, Weihai 264200, China;

[d] National Institutes for Food and Drug Control, Beijing 100050, China.

[*]**Corresponding Author.** Center for Drug Delivery System, Shanghai Institute of Materia Medica, Chinese Academy of Sciences, No. 501 of Haike Road, Shanghai 201203, China. Tel: +86 21 20231980;

[**]**Corresponding Author.** School of Pharmacy, Department of Pharmaceutics, Shenyang Pharmaceutical University, 103 Wenhua Road, Shenyang 110016, China. Tel: +86 24 23986365;

E-mail: jwzhang@simm.ac.cn (J. Zhang); slx04@163.com (L. Sun);Yinxianzhen0001@163.com (X. Yin).

Abstract

The shapes of particles and their distribution in tablets, controlled by pretreatment and tableting process, determine the pharmaceutical performance of excipient like lubricant. This study aims to provide deeper insights to the relationship of the morphology and spatial distribution of stearic acid (SA) with the lubrication efficiency, as well as the resulting tablet property. Unmodified SA particles as flat sheet-like particles were firstly reprocessed by emulsification in hot water to obtain the reprocessed SA particles with spherical morphology. The three-dimensional (3D) information of SA particles in tablets was detected by a quantitative and non-invasive 3D structure elucidation technique, namely, synchrotron radiation X-ray micro-computed tomography (SR-μCT). SA particles in glipizide tablets prepared by using unmodified SA (GUT), reprocessed SA (GRT), as well as reference listed drug (RLD) of glipizide tablets were analyzed by SR-μCT. The results showed that the reprocessed SA with better flowability contributed to similarity of breaking forces between that of GRT and RLD. SA particles in GRT were very similar to those in RLD with uniform morphology and particle size, while SA particles in GUT were not evenly distributed. These findings not only demonstrated the feasibility of SR-μCT as a new method in revealing the morphology and spatial distribution of excipient in drug delivery system, but also deepened insights of solid dosage form design into a new scale by powder engineering.

Keywords

stearic acid; morphology; spatial distribution; SR-μCT; glipizide tablets

1. Introduction

Excipients play an important role in the properties and performance of the final formulation of solid dosage forms, such as texture, stability, release, and bioavailability [1-3]. Among all the excipients, lubricant can significantly change the dynamics of blending, compression and the mechanical properties of compacts. The physical properties of lubricant such as magnesium stearate, stearic acid (SA) and talc can affect their performance in tablet and capsule formulations [4]. For pharmaceutical operations such as blending, roller compaction, tablet manufacturing and capsule filling, lubricants improve the flowability of blends, facilitate unit operations and powder processing properties by reducing the inter-particle friction [5, 6]. In terms of the effect of lubricant particle properties, SA can improve density, stickiness, and flowability of powdered excipient-drug mixtures. SA with a large surface area and small particle size has the best lubrication efficiency, since the increase of surface area can provide more surface coverage [4, 7]. Ingredient spatial distribution is closely related to the quality attribute of tablet [8, 9]. To study the influence of SA on the physical properties of tablets, it should be verified that lubricant particles are homogeneously mixed with the rest constituents of the formulation [10]. Systematic studies of three-dimensional (3D) material distribution in solid dosage forms are restricted with limited techniques. Most of the existing researches using near-infrared chemical imaging, Raman imaging or Terahertz time-domain reflection spectroscopy have been confined to research the material distribution on the surface of a sample or the cross-sectional specimen [11, 12].

Recently, innovative research of synchrotron radiation X-ray micro-computed tomography (SR-μCT) in conjunction with liquid chromatography enables materials spatial distribution visualization in tablets [13].

SR-μCT is an advanced tomographic imaging technology which employs synchrotron radiation, the most intense artificial source of X-ray, as an illuminating source to obtain the internal and micro-structural details of a solid sample at micrometer scale. Methods combining the obtained X-ray tomography, image processing, and 3D reconstruction have been devised and evaluated to study systematically the researched objects. As SR-μCT can reveal the morphology and internal 3D structure, and give a better understanding of the properties of different materials, it has been used to extensively study geological specimens [14, 15], bio-materials [16], tablets [17, 18] and granules [19]. In contrast to conventional techniques, SR-μCT provides a non-invasive scan, quantitative visualization and evaluation of the 3D structures with high-speed imaging, intensive strength and high spatial resolution. Within pharmaceutical material science and drug delivery system research, SR-μCT has been applied to analyze the complex structural systems of HPMC-based extended release tablets and gain improved mechanistic knowledge on drug release [20]. For excipients in common use like microcrystalline cellulose, the high spatial resolution of SR-μCT makes it possible to evaluate individual structure of particles, processing behavior and to classify microcrystalline celluloses of the same grade from different manufacturers [21].

This study details multi-dimensional comparative research of SA particles in the reference listed drug (RLD) of glipizide tablet (Glucotrol®, 5 mg), glipizide tablet prepared using unmodified SA (GUT) and reprocessed SA (GRT). Considering the potential influence of morphology and size of SA particles on spatial distribution and tablet properties, efforts have been made to reprocess the common SA as flat sheet-like particles into SA particles with regular spherical morphology. SA particles, before and after being compressed into tablets, have been visualized and quantified in multi-dimension to verify the effect of SA morphology on tablet quality.

2. Materials and methods

2.1. Materials

Glipizide tablet (Glucotrol®, 5 mg), manufactured by Pfizer U.S. Pharmaceuticals Group (New York, USA), was the reference listed drug (RLD). Stearic acid (≥ 99.5%, SA) and silicon dioxide (≥ 99.0%) were purchased from Huzhou Prospect Pharmaceutical Co., Ltd. (Zhejiang, China). Lactose (≥ 99.5%), microcrystalline cellulose (≥ 99.0%, MCC) and starch (≥ 99.5%) were produced by Shanghai Yunhong Pharmaceutical Excipients Co., Ltd. (Shanghai, China). Glipizide (≥ 99.5%) and sodium lauryl sulfate (≥ 99.0%, SLS) were supplied by Sinopharm Chemical Reagent Co., Ltd (Shanghai, China.). Pure water was produced by water purification system (Academic, Millipore, USA).

2.2. Reprocessing SA particles

About 300 mg SLS was weighed and dissolved under ultrasonic agitation for 10 min in 150 ml pure water to get a solution (0.2%, w/v). Then, 15 g SA was added into the SLS solution. The system was moved directly to a magnetic heated stirrer (ETS-D5, IKA, Germany) at a rotor speed of 1000 rpm and controlled at 80 ^{o}C for half an hour (The melting point of SA is 68.8 ^{o}C). After that, the obtained emulsion of liquid SA and water was transferred to a vertical overhead stirrer (10M/M-D15, IKA, Germany) to stir at 1000 rpm. At the same time, pure water (600 ml at 0 ^{o}C) was rapidly poured into the system which resulted in a sudden fall in temperature below the melting point of SA. The stir was prolonged further for 40 min. The solid particles were collected by filtration with 0.45 μm millipore filter and washed with 50 ml pure water. The obtained SA particles were dried in a desiccator for 24 h and sieved through 100 mesh size to obtain reprocessed SA particles.

2.3. Flowability research of SA particles

Unmodified SA particles were firstly sieved through 100 mesh size and the obtained ones were used for the determination of flowability and tableting. The angle of repose of unmodified SA particles and reprocessed SA particles were measured using a powder tester (PT-S, Hosokawa Micron, Co., Ltd., Shanghai, China). For each kind of SA particles, the measurement of angle of repose was analyzed in triplicate.

2.4. Preparation of glipizide tablets and determination of mass and breaking force

From the label of Glucotrol® tablet published on the Food and Drug Administration, inert ingredients used were SA, silicon dioxide, lactose, MCC and starch. Unmodified SA particles or reprocessed SA particles (1.5%, w/w) were well blended with glipizide and other excipients specified in the prescription by a bench-top mixer (VH-2, Tianhe Machinery, Co., Ltd., Shanghai, China). Tablet compaction experiments were conducted on a bench-scale rotary tablet presser (ZPS8, Tianjiu Machinery factory, Shanghai, China) equipped with 8.0 mm diameter and shallow concave punches, using compression force as 5KN. Force-measuring equipment was connected to strain gauges (RFS150E, Huqin Equipement, Shanghai, China) which allowed the pressure forces on the upper and under punches to be followed. The turret speed was set as 8 rpm. The filling depth of material was 5.60 mm. Mixed blend was directly compressed into ~198 mg tablets with thickness of 3.80 ± 0.18 mm and diameter of 7.62 mm. GUT and GRT were produced, at the same time, die wall force and ejecting force of each tablet were also recorded for further analysis.

The determination of mass was performed by weighing each kind of tablet with an analytical balance (CPA225D, Sartorius, Germany). According to the hardness test approved by USP (1217), the breaking force of RLD, GUT and GRT were measured with a hardness tester (YPD-200C, Hengqin Instrument Equipment Co., Ltd. Shanghai, China) by compressing the tablets between two slowly moving jaws until they were crushed. The mass and breaking force of each kind of glizipide tablet were measured from 6-tablet samples.

2.5. Isolation of SA particles in tablets

SA (specific gravity (s.g.): 0.86 at 20 ^{o}C) is practically insoluble in water and less dense than water. Lactose and starch are water soluble, and glipizide (s.g.: 1.29), silicon dioxide (s.g.: 2.20) and MCC (s.g.: 1.27-1.60) used in tablet are denser than water (all the data come from *PubChem*). Hence, according to the difference of solubility and density, SA particles can be separated from the tablet in water system, keeping their morphology and particle size unchanged.

SA particles in RLD, GUT and GRT were isolated from active pharmaceutical ingredient (API) and other excipients by physical method without changing their morphology. For each kind of glipizide tablet, three tablets were dipped into 10 ml ice cold water (0 ^{o}C). The tablets swelled slowly and disintegrated in 10 min. Meanwhile, ingredients were found floating up in clusters. The suspension was allowed to set for another 10 min at low temperature (0-10 ^{o}C) so that SA particles could float in water completely. The buoyant layer, about one-third of the suspension, was collected into a beaker. Then cold water (0 ^{o}C) was added to the beaker up to 20 ml. After setting for 10 min, some ingredients were found at the bottom and extremely fine particles of SA floated on the water surface. The buoyant layer was collected again and the same procedures were repeated three times to isolate pure SA particles. The finally collected buoyant layer was transferred to an evaporating dish and placed in a desiccator at 20 ^{o}C till fully dried.

2.6. Conventional morphological characterization

Morphological characterization of SA particles was carried out by scanning electron microscopy (SEM, S-4800, Hitachi). To obtain SEM photographs, specimens were evenly immobilized on a metal stub with double-sided adhesive tape and coated with a thin layer of gold before being observed under magnification.

2.7. Tablet structure measurement by SR-μCT

SR-μCT tomographic images of three kinds of glipizide tablets were acquired with the BL13W1 beam line at Shanghai Synchrotron Radiation Facility (SSRF). Glipizide tablets were fixed on the sample stage with a double-sided adhesive tape to prevent any unexpected movements during scans. Axis adjustment of the sample stage was also taken to make sure that there was no deviation in the horizontal direction during sample rotation. RLD, GUT and GRT were measured in different SR-μCT scans. According to the preliminary experiments and references, the imaging parameters have been optimized [23]. The tablets were scanned with a photon energy of 18.0 keV. After penetration through the sample, the X-rays were converted into visible light by a YAG: Ce scintillator (200 μm thickness). Projections were magnified by diffraction-limited microscope optics (1.25 × magnification) and digitized in high-resolution with an effective pixel size of 5.2 μm (ORCA Flash 4.0 Scientific CMOS, Hamamatsu K.K., Shizuoka Pref., Japan, physical pixel size: 6.5 μm). The exposure time affects the X-ray photon number reaching the detector. When the exposure time increases, the flux used to capture a projection will be raised, as well as the analyzing time. In our study, the exposure time was 1 s. The distance between sample to detector (DSD) is also a key factor in in-line phase contrast SR-μCT, and

especially useful for the imaging of materials with low-Z elements and low-density. In order to enhance the contrast to show a small difference in density, the DSD was also adjusted appropriately and was set at 12 cm. For each acquisition, 900 projection images were captured with an angular step size of 0.2° for 180°. Flat-field images (i.e., X-ray illumination on the beam path without the sample) and dark-field images (i.e., X-ray illumination off) were also collected during each acquisition procedure, so as to correct the electronic noise and variations in the X-ray source brightness. Imaging acquisition time for each CT scan was 30 min.

2.8. 3D structure reconstruction

In order to enhance the quality of reconstructed slices, propagation-based phase-contrast extraction was successfully conducted as described previously in our report [24]. Software PITRE (Phase-sensitive X-ray Image processing and Tomography REconstruction), which extracts information of diffraction enhanced imaging, and PITRE BM (PITRE Batch Manager), which executes a series of tasks that created via PITRE [25], were applied to allow parallel-beam tomography reconstruction for conventional absorption CT information. Depending on the magnitude of X-ray absorption for different materials of the glipizide tablet, gray level images were formed and the gray levels of various materials were determined, such that the SA particles of interest could be extracted from the 3D models by segmentation in imaging processing. Threshold was defined and certain gray value corresponding to the SA particles was determined (Fig. 3), so that SA particles can be separated from the solid matrix. The 3D rendered data were analyzed by using the

commercially available software-Amira (version 6.01, FEI, USA) and Image Pro Analyzer 3D (version 7.0, Media Cybernetics, Inc., Bethesda, MD, USA), to obtain structural and morphological information of SA particles in tablets. In line with the differences of materials in densities and molecular properties (Table S1), the precise profile parameters were calculated.

3. Results and discussion

3.1. Two dimensional morphology analysis of SA particles

The morphology and surface characteristics of unmodified SA particles and reprocessed SA particles analyzed by SEM are presented in Fig. 1. Notably, unmodified SA particles (Fig. 1A-C) with flat sheet-like morphology are conspicuously varied in size, while reprocessed SA particles (Fig. 1D-F) are topographically more spherical and relatively more uniform in size. At individual particle level, some particles of unmodified SA are larger in size with a smooth surface, while some of reprocessed SA particles possess obscure invagination. In short, the morphology and size of reprocessed SA particles are more regular than those of unmodified SA particles. The comparatively big differences existing in unmodified and reprocessed SA particles make them distinguishable from each other.

SEM images of SA particles isolated from RLD (Fig. 1G), GUT (Fig. 1H) and GRT (Fig. 1I) display similar appearance. Dramatic changes can be seen in the morphology of unmodified SA in GUT from an irregular flat shape to much rounder morphology, while no evident morphology changes are observed from reprocessed

SA. Due to the low melting point of SA (68.8 ^{o}C), morphological changes of SA particles could be due to the heat production process of material mixing or tableting. The more uniform of the SA particles morphology, the more uniform force applied to SA, and the smaller frictional force among materials.

SA particles were isolated according to the density and water solubility of each substance that formed the tablet, which were further confirmed by thermal platform microscope in our work and more relevant researches will be carried out in later studies.

3.2. Glipizide tablets measured by SR-μCT

By SR-μCT scan, original data of hundreds of shadow projections were firstly gotten (Fig. 2A) but revealed no useful information. Phase retrieval was performed with projection images using the software PITRE for propagation-based phase contrast extraction (Fig. 2B). Then, reconstructed 2D slices of the specimen were obtained and the value of α was calibrated from 32 bit to 8 bit (gray value 0-255) (Fig. 2C and 2D). The CT image values (gray-levels) provide information on the material X-ray attenuation coefficient at each point in the image. As the reconstructed 2D slice (Fig. 3A) of the RLD radial middle layer show, the lighter areas of the slice has a relatively high gray value and darker areas with a low gray value. SA particles have the lowest density among all the ingredients in glipizide tablet, which reflects weaker X-ray absorption and the lowest gray value. Thus, it is certained that the small dark spots in the slice are the SA particles. Fig. 3B is the partial magnification of the slice,

which shows how the threshold of SA particles defined. As shown in the line profile (Fig. 3C) of the selected SA particle, the steepest part of the line was chosen and the middle value of its vertical coordinate was determined as the threshold. In order to obtain as exact gray value of SA particles as possible, the dark spots in different slices of different glipizide tablets were calculated. As the threshold was defined and certain gray value corresponds to the SA particles was determined, SA particles can be separated from the solid matrix (Fig. 2F), which realistically reconstructs the morphology and position of SA particles in tablet.

Then, all the 2D slices were processed by Amira to get the full reconstructed 3D images of tablets (Fig. 2E). The 3D morphological information of hundreds even thousands of SA particles can be obtained and 3D quantitative parameters are calculated. Besides, the uniformity of SA particles spatial distribution in tablets is monitored via high-resolution imaging using SR-μCT.

The use of non-destructive X-ray micro-tomography allows one to characterize the density distribution of an individual tablet and then further characterize the particles within the tablet. The optimized 3D models provide full details of surface morphology and distribution of SA particles in the tablet. 3D images of SA particles existed in tablets are presented from two different perspectives (Fig. 4A, 4C and 4E). Partial magnifications of SA particles are also displayed (Fig. 4B, 4D and 4F) and each particle is colored randomly by Image Pro Analyzer 3D. The mapping spatial distribution of SA particles from 3D overall view shows that SA particles in RLD (Fig. 4A and 4B) and in GRT (Fig. 4E and 4F) are uniformly distributed. In some parts of

GUT (Fig. 4C and 4D), there are SA clusters and some zones are without SA particles, reflecting that spatial distribution of SA particles is relatively heterogeneous in GUT. This phenomenon suggests that the inter-particle friction varied greater among different parts in GUT when compared with RLD and GRT. The size of SA particles in RLD and GRT is more regular than in GUT. Moreover, SA particles exhibit most standard morphology in GRT, followed by in RLD and then in GUT, which can be seen from partial magnifications (Fig. 4B, 4D and 4F). Apparently, the size of SA particles in GUT is less regular, and the difference of morphological characteristics between different particle size ranges is also big. Bigger SA particles may also result from the agglomeration of the particles in GUT, which most likely due to the different SA particles used. With the powerful SR-μCT technology, physical state of SA particles located in solid dosage form is visualized from multiple vision perspectives with a high spatial resolution.

3D morphological parameters like sphericity, equivalent diameter, area of surface, volume, total area of surface of SA particles, as well as number of SA particles in the three kinds of tablets were calculated and tabulated in Table 1. The frequency distributing graphs of sphericity and surface area of SA particles in each kind of tablet are also shown in Fig. 5 to visually compare the differences by mathematical statistics. Sphericity is usually defined as a ratio of the surface area of a sphere having the same volume with the particle to the actual surface area of the particle [26]. The sphericity of a sphere is “1” and any particle which is not a sphere will have sphericity less than “1” [27]. Average value of sphericity for SA particles in GRT is similar to that in RLD,

while it is smaller in GUT. Both the standard deviation of sphericity and the frequency distributing graph of the sphericity (Fig. 5A) indicate the sphericity fluctuation of SA particles in GRT is the smallest. What's more, the morphology of SA particles in GUT is the most non-uniform, which is clearly presented in the frequency distributing graph of sphericity. As sphericity of particles is thought to be related to the flowability [4], SA particles used in GRT and RLD have better lubrication efficiency than those in GUT. In addition, the improved sphericity of SA particles in GRT is undoubtedly owing to the reprocessing.

Equivalent diameter here is the diameter of a sphere with the same volume as the target object. The average value of equivalent diameter for SA particles in GRT is the smallest, while the standard deviation of equivalent diameter for SA particles in GUT is the biggest. Meanwhile, for average value of surface area and volume, SA particles in GRT, RLD and GUT arise by their turns. Therefore, it is easy to conclude that SA particles in GRT are relatively small. Because the usage amount of SA in GUT and GRT is the same, the smaller particle size contributes to larger number of particles. And the number of SA particles in GRT is the biggest, then in RLD, and followed by SA particles in GUT. Since the standard deviations of size parameters especially those of SA particles in GUT are so high, considering the average value of size parameters alone is not enough to get accurate information. As mentioned earlier, larger surface area contributes to improved lubrication efficiency. The total surface area of SA particles in GUT is the smallest, reflecting that SA particles with biggest particle size in GUT have no better lubrication efficiency than those in the other two kinds of

tablets. The frequency profiles (Fig. 5B) of surface area indicate that rather than in GUT, the frequency distribution tendency of SA particles in GRT are more similar with in RLD. In short, from the 3D measurement using SR-μCT technology, uniformly spherical SA particles with a narrow size distribution can be observed in GRT, which is closer to the results in RLD. The elaborate quantitative results of SA particles in tablet, which cannot be obtained without the powerful 3D visualization tool, clearly have a profound significance for pharmaceutical design.

Rather than the conventional microscopic evaluations only revealing incomplete morphology, the 3D structural and morphological elucidation technique of SR-μCT can satisfy the research requirements with reliable and comprehensive information in drug delivery system. Furthermore, the degree of fluctuation shown in standard deviations of 3D parameters is a reflection of the regularity in morphology. It is found that SA particles in GRT feature the best regular morphology that show superior flowability. SA particles in GUT have the highest fluctuation range in morphology. Particularly, for surface area and volume, standard deviations of SA particles in GUT are much higher than those in the other two kinds of tablets. The dramatic visualization of SR-μCT images offered a reliable semi-quantitative overview of the SA particles distribution in tablets. Overall, compared with SA particles in GUT, those in GRT are more consistent with RLD.

As demonstrated by the excipient example presented in this report, accurate quantitative characterizations of component in tablet are possible when appropriate techniques are used. For SR-μCT, high spatial resolution and contrast imaging form

the basis of reliable quantitative analysis. The spatial resolution in our study is 5.2 μm and SA particles below 5.2^3 μm^3 cannot be determined. The accuracy of the quantified SR-μCT experiments also depends on the stability of X-ray beam physical dimensions and intensity profile, the detection response characteristics and count rate ranges.

3.3. Flowability, compression property and breaking force analysis

The angle of repose for unmodified SA particles and reprocessed SA particles are 52.61 ± 0.90^o and 49.08 ± 1.23^o, respectively. For optimized SA particles, its average value of angle of repose is smaller, reflecting its better flowability than unmodified SA particles. What's more, the existence of the trace amount of SLS brings no improvement in the flowability of SA particles (data are not be provided). Average value of die wall force of GUT and GRT are 0.41kN and 0.47kN, and ejecting force are 0.23kN and 0.17kN, respectively. The die wall force indicates favorable compaction properties that prevent problems such as capping during mass manufacturing of tablets [28], the higher die wall force for GRT indicates that reprocessed SA particles are more suitable for tableting. For ejecting force, contrasted to unmodified SA particles, reprocessed SA particles make the tablet formulation possess lower adhesive force and frictional force during ejection of GRT from the die cavity. Tablet breaking force is a critical parameter in pharmaceutical process quality control, and depends on factors such as compression force, particle size and inter-particle force [29]. In our research, breaking force evolution for RLD (70.59 ± 6.82 N), GUT (86.58 ± 7.91 N) and GRT (68.09 ± 4.24 N) indicates that the effect of SA particles on the breaking force of tablet is obvious. The breaking force increased

with the degree of irregularity of SA particles and GRT is much closer to RLD. Combined with the SR-μCT analysis, it seems that more regular morphology with higher sphericity of SA particles resulted in a less inter-particle force and decreased breaking force. It should be noted that the gap of morphological parameters like particle volume, surface area and total surface area between GRT and RLD are large, but the breaking force of RLD and GRT are overlapping. While more importantly, the order of these morphological parameters of RLD, GRT and GUT has the same trend as that of the breaking forces of the three kinds of tablets considering the mean ± SD values. Some complicated mathematical or logical relationship may exist between these morphological parameters and breaking force. After all, it has been confirmed that the breaking force of tablets is affected by multiple factors, and the specific mathematical relationship has not been reported so far. It is thought that the usage of different kinds of SA particles chiefly contributed to the morphological differences among SA particles in RLD, GUT and GRT and resulted in difference in tablet breaking force, whereas the compaction conditions may also have impact on the results that cannot be underestimated. More detailed analyses of these impacts are beyond the scope of the present report but deserve further investigation.

4. Conclusions

In this study, a powerful structural method has been established for the characterization of morphology and spatial distribution of SA particles in tablet prepared with different morphologies of SA as a new way to research the material in solid dosage forms. The improved structural consistency between reprocessed SA

particles in GRT and SA particles in RLD ensures high quality of glipizide tablets. For excipients like SA to function according to its particle structure and spatial distributions in tablets, 3D reconstruction and quantitative structure analysis by SR-μCT significantly deepen insights of solid dosage form design and evaluation as well as rational optimization of production process. More specifically, the novel methodology of excipient structure consistency research opens a new way to secure high quality for both generic and brand products of drugs in solid dosage forms.

Acknowledgements

The authors are grateful for the financial support from the National Science and Technology Major Project (2017ZX09101001-006). Thanks to the BL13W1 beamline of the SSRF for the precious beam time and help from the team.

Declaration of interest

The authors report no conflicts of interest. The authors alone are responsible for the content and writing of this article.

Reference

[1] Matsuda Y, Minamida Y, Hayashi S. Comparative evaluation of tablet lubricants - effect of application method on tablet hardness and ejectability after compression. J Pharm Sci 1976;65(8):1155-60.

[2] Shojaee S, Kaialy W, Cumming KI, Nokhodchi A. Comparative evaluation of drug release from aged prolonged polyethylene oxide tablet matrices: effect of excipient and drug type. Pharm Dev Technol 2016;21(2):189-95.

[3] Villalobos JR, Villafuerte RL. Effect of carrier excipient and processing on stability of indorenate hydrochloride/excipient mixtures. Pharm Dev Technol 2001;6(4):551-61.

[4] Li JJ, Wu YM. Lubricants in pharmaceutical solid dosage forms. Lubricants 2014;2(1):21-43.

[5] Fridrun P, Mia Y. The influence of particle size and shape on the angle of internal friction and the flow factor of unlubricated and lubricated powders. Int J Pharm 1996;144(2):187-94.

[6] Wang J, Wen H, Desai D. Lubrication in tablet formulations. Eur J Pharm Biopharm 2010;75(1):1-15.

[7] Barra J, Somma R. Influence of the physicochemical variability of magnesium stearate on its lubricant properties: possible solutions. Drug Dev Ind Pharm 1996;22(11):1105-20.

[8] Amigo JM, Ravn C. Direct quantification and distribution assessment of major and minor components in pharmaceutical tablets by NIR-chemical imaging. Eur J Pharm Sci 2009;37(2):76-82.

[9] Sando G, Dubois J. "Seeing" the chemicals in pharmaceutical tablets with NIR chemical imaging. Chim Oggi 2010;28(1):40-2.

[10] Perrault M, Bertrand F, Chaouki J. An experimental investigation of the effect of the amount of lubricant on tablet properties. Drug Dev Ind Pharm 2011;37(2):234-42.

[11] Wu Z, Tao O, Cheng W, Yu L, Shi X, Qiao Y. Visualizing excipient composition and homogeneity of compound liquorice tablets by near-infrared chemical imaging. Spectrochim Acta A Mol Biomol Spectrosc 2012;86(86):631-6.

[12] Takeuchi I, Shimakura K, Ohtake H, Takayanagi J, Tomoda K, Nakajima T, et al. Nondestructive analysis of structure and components of tablet coated with film by the usage of terahertz time-domain reflection spectroscopy. J Pharm Sci 2014;103(1):256-61.

[13] Zhang L, Wu L, Wang CF, Zhang GQ, Yu L, Li HY, et al. Synchrotron radiation micro-computed tomography-guided chro-matographic analysis displays the material distribution in tablets. Anal Chem 2018;90(5):3238-44.

[14] Altman SJ, Uchida M, Tidwell VC, Boney CM, Chambers, BP. Use of X-ray absorption imaging to examine heterogeneous diffusion in fractured crystalline rocks. J Contam Hydrol 2004;69(1-2):1-26.

[15] Tomioka S, Kozaki T, Takamatsu H, Noda N, Nisiyama S, Kozai N, et al. Analysis of microstructural images of dry and water-saturated compacted bentonite samples observed with X-ray micro CT. Appl Clay Sci 2010;47(1):65-71.

[16] Zhang MQ, Zhou L, Deng QF, Xie YY, Xiao TQ, Cao YZ, et al. Ultra-high-resolution 3D digitalized imaging of the cerebral angioarchitecture in rats using synchrotron radiation. Sci Rep 2015;5:14982

[17] Laity PR, Cameron RE. Synchrotron X-ray microtomographic study of tablet swelling. Eur J Pharm Biopharm 2010;75(2):263-76.

[18] Li H, Yin X, Ji J, Sun L, Shao Q, York P, et al. Microstructural investigation to the controlled release kinetics of monolith osmotic pump tablets via synchrotron radiation X-ray micro-tomography. Int J Pharm 2012;427(2):270-5.

[19] Crean B, Parker A, Le Roux D, Perkins M, Luk SY, Banks SR, et al. Elucidation of the internal physical and chemical microstructure of pharmaceutical granules using X-ray micro-computed tomography, Raman microscopy and infrared spectroscopy. Eur J Pharm Biopharm 2010;76(3):498-506.

[20] Yin XZ, Li HY, Guo Z, Wu L, Chen FW, Shao Q, et al. Quantification of swelling and erosion in the controlled release of a poorly water-soluble drug using synchrotron X-ray computed micro-tomography. AAPS J 2013;15(4):1025-34.

[21] Fang LW, Yin XZ, Wu L, He YP, He YZ Qin W, et al. Classification of microcrystalline celluloses via structures of individual particles measured by synchrotron radiation X-raymicro-computed tomography. Int J Pharm 2017;531(2):658-67.

[22] Ren YQ, Chen C, Chen RC, Zhou GZ, Wang YD, Xiao TQ. Optimization of image recording distances for quantitative X-ray in-line phase contrast imaging. Opt Express 2011;19(5): 4170-81.

[23] Yang S, Yin XZ, Wang CF, Li HY, He Y, Xiao TQ, et al. Release behaviour of single pellets and internal fine 3D structural features co-define the *in vitro* drug release profile. AAPS J 2014;16(4): 860-71.

[24] Guo Z, Yin XZ, Liu CB, Wu L, Zhu WF, Shao Q, et al. Microstructural investigation using synchrotron radiation X-ray microtomography reveals taste-masking mechanism of acetaminophen microspheres. Int J Pharm 2015;499(1-2):47-57.

[25] Chen RC, Dreossi D, Mancini L, Menk R, Rigon L, Xiao TQ. PITRE: software for phase-sensitive X-ray image processing and tomograph y reconstruction. J Synchrotron Radiat 2012;19(5):836-45.

[26] Barksdale RD, Kemp MA, Sheffield WJ, Hubbard JL. Measurement of aggregate shape, surface area, and roughness. Transportation Research Record1301, National Research Council, Washington, 1991. p.107-16.

[27] Mora CF, Kwan KH. Sphericity, shape factor, and convexity measurement of coarse aggregate for concrete using digital image processing. Cem Concr Res 2000;30(3):351-8.

[28] Kasa P, Bajdik J, Zsignond Z, Pintye-Hodi K. Study of the compaction behaviour and compressibility of binary mixtures of some pharmaceutical excipients during direct compression. Chem Eng Process 2009;48(4):859-63.

[29]Javaheri H, Carter P, Elkordy AA. Wet granulation to overcome liquisolid technique issues of poor flowability and compactibility: a study to enhance glibenclamide dissolution. J Pharm & Drug Develop 2014;2(3):1-12.

Figures：

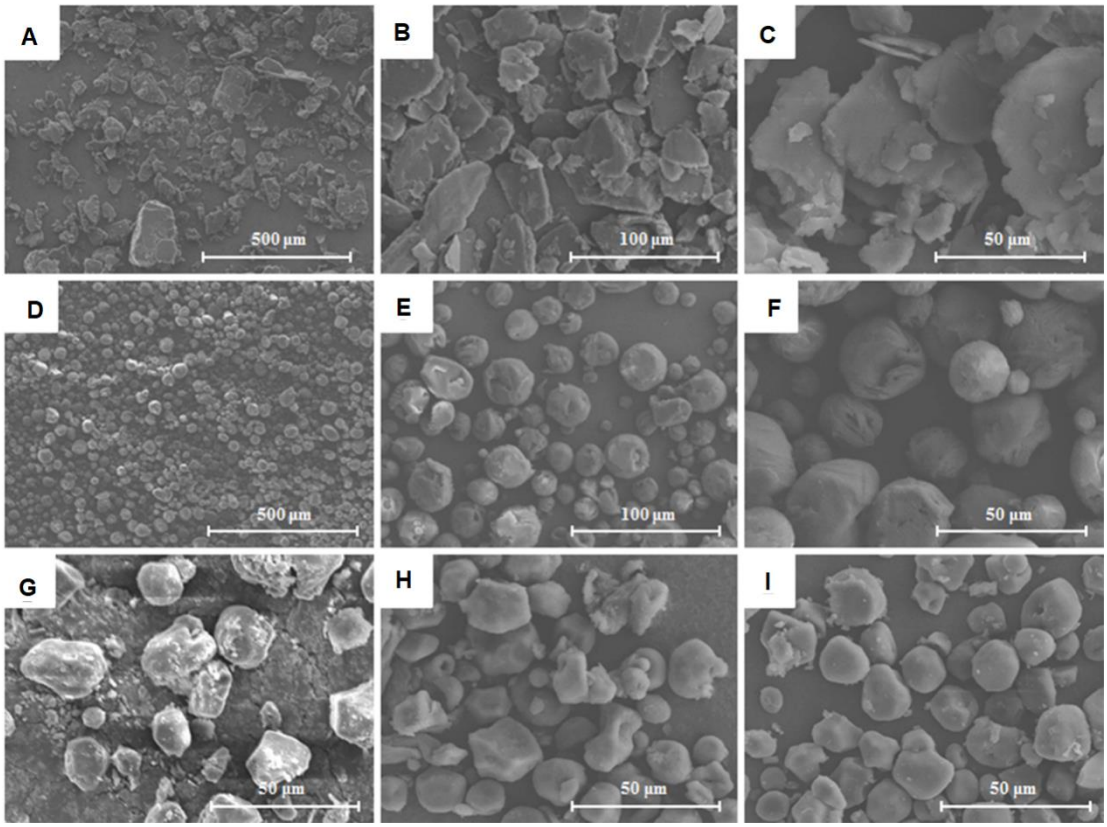

Fig. 1. SEM micrographs of unmodified SA (A-C) and reprocessed SA (D-F) under different magnifications reveal that the morphology and size of reprocessed SA are more regular than those of unmodified SA. SEM images of SA particles isolated from RLD (G), GUT (H) and GRT (I) show that the morphologies of these three kinds of SA particles are similar.

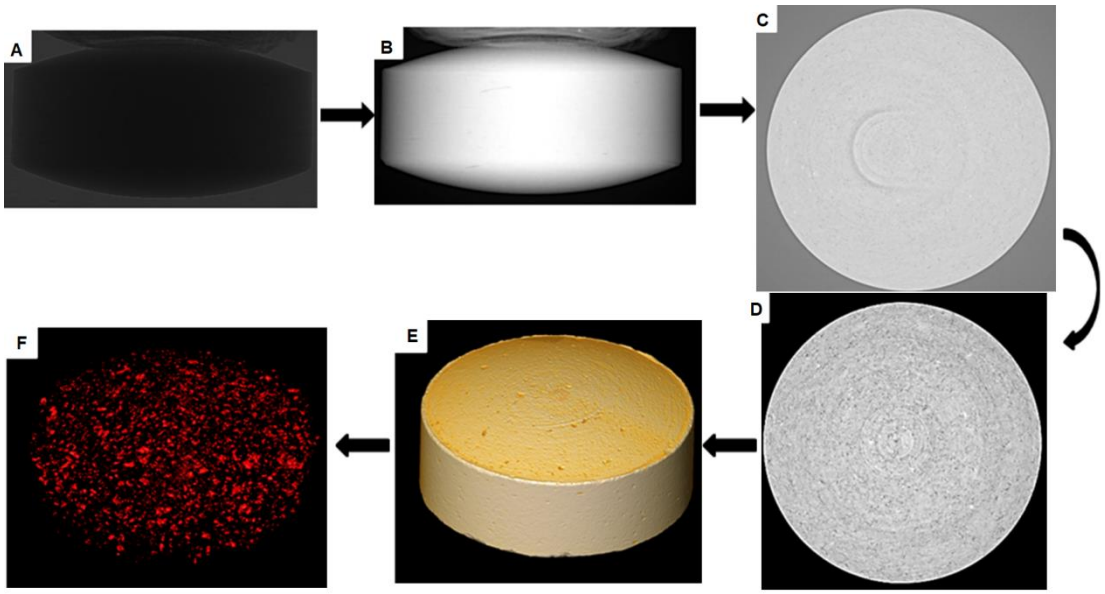

Fig. 2. Reconstruction and phase contrast extraction process include shadow projection after flat-field and dark-field corrections (A), projection after phase retrieval (B), reconstructed slice (C), truncated slice (D), 3D image of a tablet (E) and SA particles in the tablet (F).

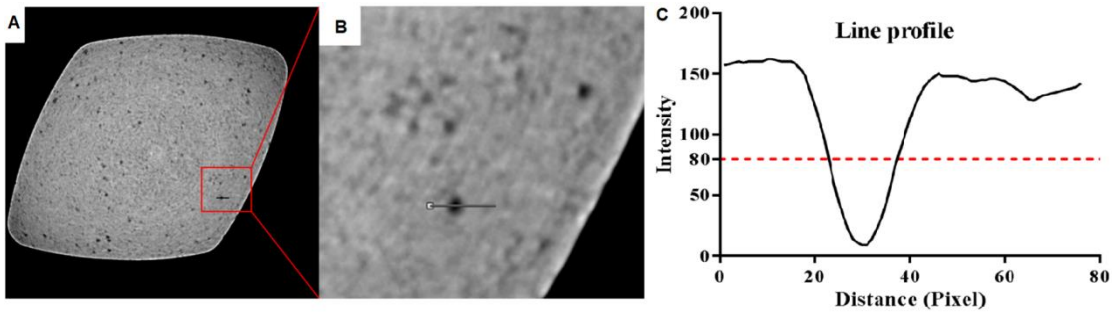

Fig. 3. 2D original slice of the radial middle layer of the glipizide tablet (A), partial magnification of the slice containing the selected SA particle (B) and the line profile of the selected SA particle (C).

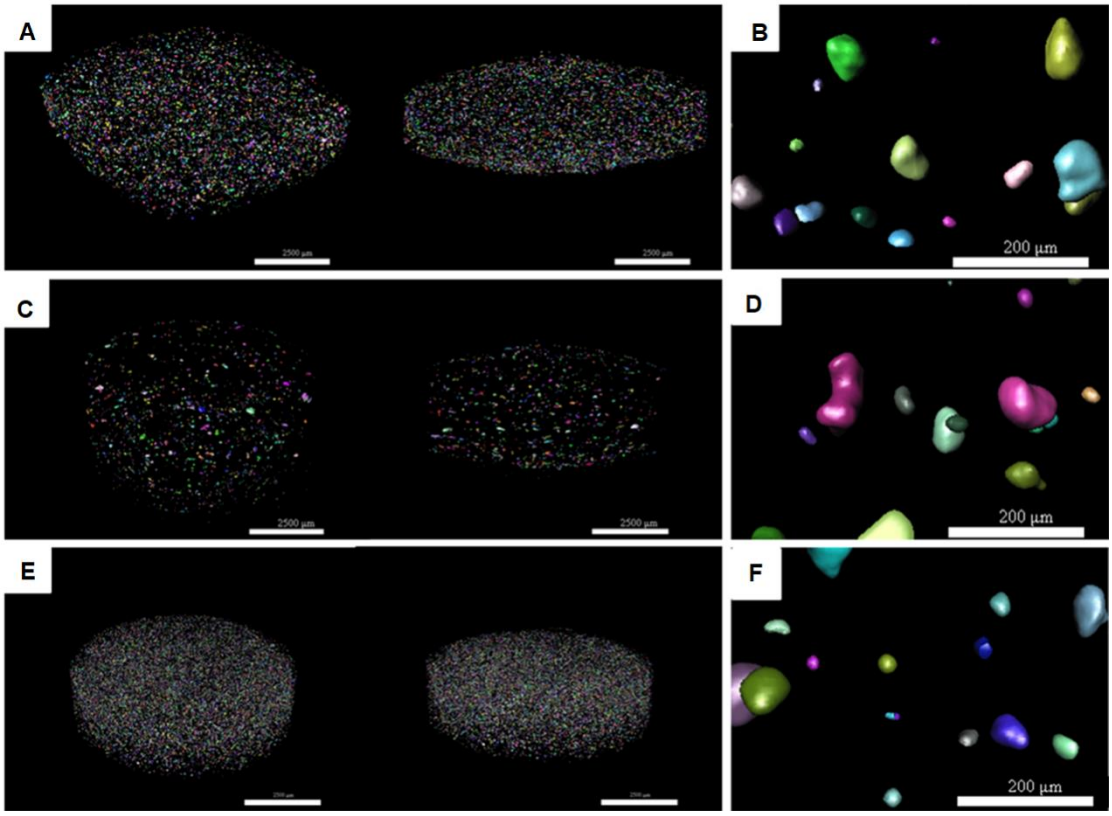

Fig. 4. The 3D images of SA particles in different kinds of glipizide tablets. The left column shows location of the total SA particles in tablets and the right column shows a partial enlarged view of SA particles. (A, B), (C, D), (E, F) represent SA in RLD, GUT and GRT, respectively. Each particle is colored randomly by the software.

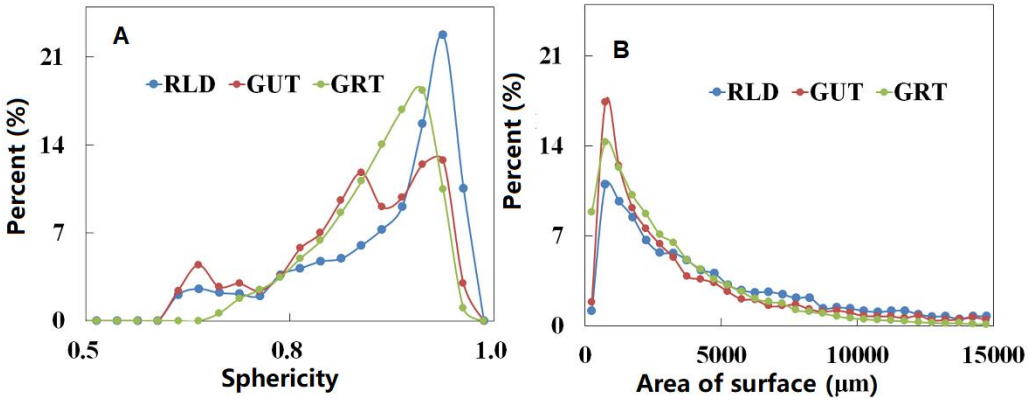

Fig. 5. Frequency distributing graphs of 3D morphological parameters of SA particles in RLD (blue), GUT (red) and GRT (green).

Tables：

Table 1 Comparison and analysis of 3D morphological parameters like sphericity, equivalent diameter, area of surface, volume, total area of surface of individual SA particles, as well as the number of SA particles in RLD, GUT and GRT (mean ± SD).

Morphology parameter	Individual SA particles in tablets		
	RLD	GUT	GRT
Sphericity	0.86 ± 0.09	0.83 ± 0.09	0.86 ± 0.06
Equivalent diameter (μm)	36.28 ± 17.84	34.60 ± 22.90	26.45 ± 11.79
Area of surface(μm^2)	5 786 ± 6 156	6 659 ± 12 644	3 086 ± 2 752
Volume(μm^3)	45 872 ± 73 025	63 381 ± 222 477	15 923 ± 20 389
Total area of surface (μm^2)	4.88×10^7	2.98×10^7	8.60×10^7
Number of particles	8 432	4 479	27 875

Graphical abstract